Theoretical analysis and simulations of strong terahertz radiation from the interaction of ultrashort laser pulses with gases

Min Chen* and Alexander Pukhov
Institut für Theoretische Physik I, Heinrich-Heine-Universität Düsseldorf, 40225, Düseldorf, Germany

Xiao-Yu Peng and Oswald Willi
Institut für Laser und Plasma Physik, Heinrich-Heine-Universität Düsseldorf, 40225, Düsseldorf, Germany
(Received 3 June 2008; published 27 October 2008)

Terahertz (THz) radiation from the interaction of ultrashort laser pulses with gases is studied both by theoretical analysis and particle-in-cell (PIC) simulations. A one-dimensional THz generation model based on the transient ionization electric current mechanism is given, which explains the results of one-dimensional PIC simulations. At the same time the relation between the final THz field and the initial transient ionization current is shown. One- and two-dimensional simulations show that for the THz generation the contribution of the electric current due to ionization is much larger than the one driven by the usual ponderomotive force. Ionization current generated by different laser pulses and gases is also studied numerically. Based on the numerical results we explain the scaling laws for THz emission observed in the recent experiments performed by Xie *et al.* [Phys. Rev. Lett. **96**, 075005 (2006)]. We also study the effective parameter region for the carrier envelop phase measurement by the use of THz generation.

DOI: 10.1103/PhysRevE.78.046406 PACS number(s): 52.59.Ye, 52.25.Jm, 52.25.Os, 52.65.Rr

I. INTRODUCTION

Novel sources of strong terahertz electromagnetic pulse emission attracted wide attention due to a number of potential applications such as THz imaging, material characterization, tomography, and so on [1,2]. Many schemes of THz generation exist [3–10], which exploit traditional nonlinear optics methods of laser medium interaction. Since the ambient air is a very convenient nonlinear medium for ultrastrong laser pulses, the THz generation by laser air interaction has been studied for many years. The first observation of THz signal in laser air interaction is by Cook *et al.* [11]. He explained it in terms of the four-wave rectification. After that, a few groups have also reported the THz generation in laser air interaction, but different explanations have been proposed [12–16]. Among those, the transient photocurrent model suggested by Kim *et al.* [17] can well explain the two-color laser pulses experiments. Earlier, Kress *et al.* [18] already used this mechanism to measure the carrier-envelope phase of few-cycle laser pulses. In the paper of Kim *et al.*, they question the four wave mixing mechanism and examine the origin of $\chi^{(3)}$, which is central in the nonlinear optics explanation. They also pointed out that only a limited pump energy range has been checked in the experiments performed by Xie *et al.* [19], in which the explanation is based on the four wave mixing mechanism.

In this paper, we restudy the ionization current model by one- and two-dimensional PIC simulations, in which the ionization subprogram has been included [20,21]. First, we provide the analytical model for the THz generation via the ionization current. Then, we demonstrate this kind of mechanism by PIC simulations. We also show the contribution from ionization electric current is much larger than the electric current driven by the usual ponderomotive force which has been studied in detail by Sprangle *et al.* [3]. After that, we calculate the ionization current generated by different laser pulses and gases. We find that the scaling laws observed in the earlier experiments can also be well explained by this model, which questions the mechanism of the nonlinear optical processes. Finally, we study the effective parameter region for the measurement of CEP for different few-cycle laser pulses.

II. ANALYTICAL MODEL WITH 1D ASSUMPTION

When the ultrashort laser pulse interacts with a neutral gas medium, it ionizes the gas first. Then the new born electrons start responding to the laser field. Unlike the electrons in the interaction of laser pulse with the usual existing plasmas, the new born electrons in the laser gas interaction can retain transverse momentum after the laser pulse passes and thus generate a net transverse current [17,22]. In this section, we deduce the THz radiation from this initially generated current assuming the one-dimensional (1D) geometry. The purpose is to explain results of the 1D PIC simulations. Further, we compare the 1D simulation results with 2D PIC simulations and point out the differences.

From the Maxwell equations, we get

$$\frac{\partial^2 \vec{E}}{c^2 \partial t^2} - \nabla^2 \vec{E} = -\nabla\left(\frac{\rho}{\epsilon_0}\right) - \mu_0 \frac{\partial \vec{j}}{\partial t}. \tag{1}$$

For the one-dimensional geometry, we have $\partial_y = \partial_z = 0$, here y and z axes are along the transverse directions, and x axis is along the laser propagation direction. If the laser pulse is initially Y polarized with the transverse electric field E_y, we get

*mchen@tp1.uni-duesseldorf.de

$$\frac{\partial^2 E_y}{c^2 \partial t^2} - \partial_x^2 E_y = -\mu_0 \frac{\partial j_y}{\partial t} \tag{2}$$

and

$$j_y = \sum_{v_y} -e n_{v_y} v_y, \tag{3}$$

where n_{v_y} is the density of electrons whose velocity is v_y. The density of the electrons n_e and the electron velocity v obey the following equations [3]:

$$\frac{dn_e}{dt} = \sum_i \omega_i n_i - \beta_{\text{recom}} n_e^2 - \beta_{\text{attach}} n_e n_{\text{gas}}^2, \tag{4}$$

$$\frac{d\vec{v}}{dt} = -\frac{e}{m}\left(\vec{E} + \frac{\vec{v} \times \vec{B}}{c}\right) - \nu_e \vec{v}. \tag{5}$$

Here the terms of $\beta_{\text{recom}} n_e^2$ and $\beta_{\text{attach}} n_e n_{\text{gas}}^2$ represent the effects of electron recombination and attachment on the gas molecules, respectively. The ADK model is used to calculate the ionization rate [23,24]

$$\omega_i = 6.6 \times 10^{16} \frac{Z^2}{n_{\text{eff}}^{4.5}} \times \left[10.87 \frac{Z^3 E_H}{n_{\text{eff}}^4 E_{\text{opt}}}\right]^{2n_{\text{eff}}-1.5} \times \exp\left[-\frac{2}{3}\frac{Z^3 E_H}{n_{\text{eff}}^3 E_{\text{opt}}}\right](\text{s}^{-1}), \tag{6}$$

where $E_H = 5.14 \times 10^9$ V/cm is the atomic unit of the electric field, E_{opt} is the electric field of the laser pulse, Z is the charge of the ionized atomic, $n_{\text{eff}} = Z/\sqrt{E_{\text{ion}}(\text{eV})/13.6}$ is the effective main quantum number of the ionized ions, and E_{ion} is the ionization potential in eV. Since the recombination and attachment time (~nsec) for the electrons are much longer than the time of ionization and THz generation process [3], we neglect both of them in our theoretical model and simulations. The electron-ion collision rate ν_e is 10^{12} s^{-1} under our condition, which corresponds to a time between collisions of ~1 ps [17]—a time much longer than the longest pulse length of 150 fs used in our simulations. On the other hand we are only interested in the first period of the THz radiation (<200 fs) which is strongest. So the collision effect is also neglected for the present study. Further more, in our theoretical model we neglect the nonlinear term in the electron motion, i.e., $\vec{v} \times \vec{B}$. It includes the ponderomotive force which is studied in detail by Sprangle *et al.* [see Eq. (7) in Ref. [3]]. As we will show later, in our condition the electric current due to initial transient ionization is much larger than the one driven by the ponderomotive force. Therefore the minor contribution of the ponderomotive force can be omitted.

With these assumptions, we obtain the final evolution equation for the transverse electric field

$$\frac{\partial^2 E_y}{c^2 \partial t^2} - \partial_x^2 E_y + \frac{\omega_p^2}{c^2} E_y = \mu_0 e \sum_{v_y} v_y \frac{\partial n_{v_y}}{\partial t} - \mu_0 e \sum_{v_y} n_{v_y} v_x \frac{\partial v_y}{\partial x}. \tag{7}$$

Here $\omega_p^2 = n_e e^2/\epsilon_0 m$ is the plasma frequency. Throughout this paper, we use the relativistically normalized amplitude of the laser electric field $a = eE_y/m\omega c$. In our applications, $|a| \ll 1$, so that the longitudinal velocity of electrons satisfies $v_x/c \ll 1$, and the second term on the right side can be neglected. The rationality of this approximation is also demonstrated by our test 1D simulations, in which we can set $v_x = 0$ and get the same results as in the ones without this setting. The first term on the right side is then the only source for the transverse oscillations and THz generation. This term can also be divided into two different contributions: the first one comes from the initial ionization current generation, since the new born electrons retain the velocity v_y after the laser passes ($\partial_t n_{v_y} \neq 0$); the second one comes from the density oscillation due to the electrons oscillation along the longitudinal direction with the plasma frequency ω_p. The second one acts as an oscillation source and makes the THz generation at the plasma frequency. However, since the longitudinal velocity is very small, $v_x/c \ll 1$, the contribution of this mechanism can be neglected as we pointed out above. Thus, the only essentially contributing source for the THz generation is the initial ionization current. In the following, we deduce the THz radiation from this initial ionization current.

We rewrite Eq. (7) to be

$$\frac{\partial^2 E_y}{c^2 \partial t^2} - \partial_x^2 E_y + \frac{\omega_p^2}{c^2} E_y = -\mu_0 j_{y0} \delta(v_{if} t - x)(t > 0) \tag{8}$$

with the initial condition $E_y(0,x) = 0$, $\partial E_y(0,x)/\partial t = 0$. Here $j_{y0}\delta(v_{if}t - x)$ represents the increase rate of the transient ionization current, v_{if} is the velocity of the ionization front. Using Fourier and Laplace integral transformation, we get the solution for E_y:

$$E_y(t,x) = -\sqrt{\frac{\pi}{2}} \frac{j_{y0}}{c\epsilon_0} \int_0^{v_{if}t} J_0\left[\omega_p \sqrt{\left(t - \frac{\xi}{v_{if}}\right)^2 - \frac{|x-\xi|^2}{c^2}}\right] \times H\left(t - \frac{\xi}{v_{if}} - \frac{|x-\xi|}{c}\right) d\xi. \tag{9}$$

Here J_0 is the zero order Bessel function and H is the Heaviside unit step function. We point out that this solution is only correct inside a plasma since we have assumed the plasma frequency ω_p^2 is uniform in the x direction as shown in the left side of Eq. (8). This field can be radiated only at the plasma boundary, or when the plasma has a density gradient, that is usually the case in experiments.

If the ionization is only taking place within the region of $0 < x < l_0$ and the time period l_0/v_{if} is much smaller than the THz period, we can get the solution for E_y

$$E_y(t,x) \simeq -\sqrt{\frac{\pi}{2}}\frac{j_{y0}}{c\epsilon_0}\int_0^{l_0} J_0\left(\omega_p\sqrt{t^2-\frac{|x-\xi|^2}{c^2}}\right) \times H\left(t-\frac{|x-\xi|}{c}\right)d\xi. \quad (10)$$

Using known properties of the Bessel function, we can get the asymptote of E_y in the limit $t \gg (x+l_0)/c$:

$$E(t,x) \approx \frac{-j_{y0}l_0}{c\epsilon_0\sqrt{\omega_p t}}\cos(\omega_p t - \pi/4). \quad (11)$$

The radiated transverse electric field is thus oscillating at the plasma frequency ω_p and the amplitude decreases with time. The maximum value is proportional to the initial ionization current j_{y0}, which gives the same results as the multi dimensional condition [22], for which the THz generation is explained by oscillating dipole mechanisms.

Up to now we have theoretically studied the THz signal in the one-dimensional geometry. It is interesting to compare the 1D results with multidimensional simulations, since the radiation can also result from the dipole oscillation in the real multi dimensional space, especially from the transverse oscillation driven by the ponderomotive force of the laser pulse. In the following sections, we make the PIC simulations to show the difference of 1D and 2D results. In the 2D simulations we use a p-polarized laser pulse, with which the transverse oscillation of the electrons can be well treated, since the transverse component of $\nabla \cdot E$ in the simulation is nonzero. At the same time we make a compared simulation in which the laser pulse interacts directly with existing plasmas. As we can see the THz signal is dramatically weakened when there is no ionization process.

III. ONE- AND TWO-DIMENSIONAL PIC SIMULATIONS

The field-ionization model in our PIC codes [20] and ionization current calculation is based on the description of tunnel ionization of complex atoms in alternating electric fields given by Ammosov, Delone, and Krainov in the form of Penetrante and Bardsley [23,24]. When neutral atoms are ionized in the PIC simulations, the freed electrons have zero velocity initially. Once the electron is released, it starts to move under action of the plasma and laser electromagnetic fields according to the Lorentz equation. The laser evolution due to ionization such as frequency shift and the ionization current generation are self-consistently included. In simulations with ionization process, the neutral He gases initially have uniform density $n_{\mathrm{He}}=0.0005n_c$ in the region $10\lambda < x < 30\lambda$, here $n_c=4\pi^2 m\epsilon_0 c^2/\lambda^2 e^2$ is the critical density for the incident laser pulse ($n_c=1.7\times10^{21}/\mathrm{cm}^3$ when the incident laser wavelength is $\lambda=800$ nm). The amplitude of the normalized electric field of the laser pulse is $a_0=0.2$ and duration $T=3T_0$, here T_0 is the period of the incident laser pulse. The laser pulse is p polarized in the 2D simulation. Figures 1(a)–1(d) shows the spatial distribution of the charge density of ions $\Sigma_i q_i n_i$, density of electrons n_e, the transverse electric field E_y, and the transverse current j_y at the time of $t=20T_0$. Figure 1(e) shows the spatial distribution of j_y at $t=30T_0$.

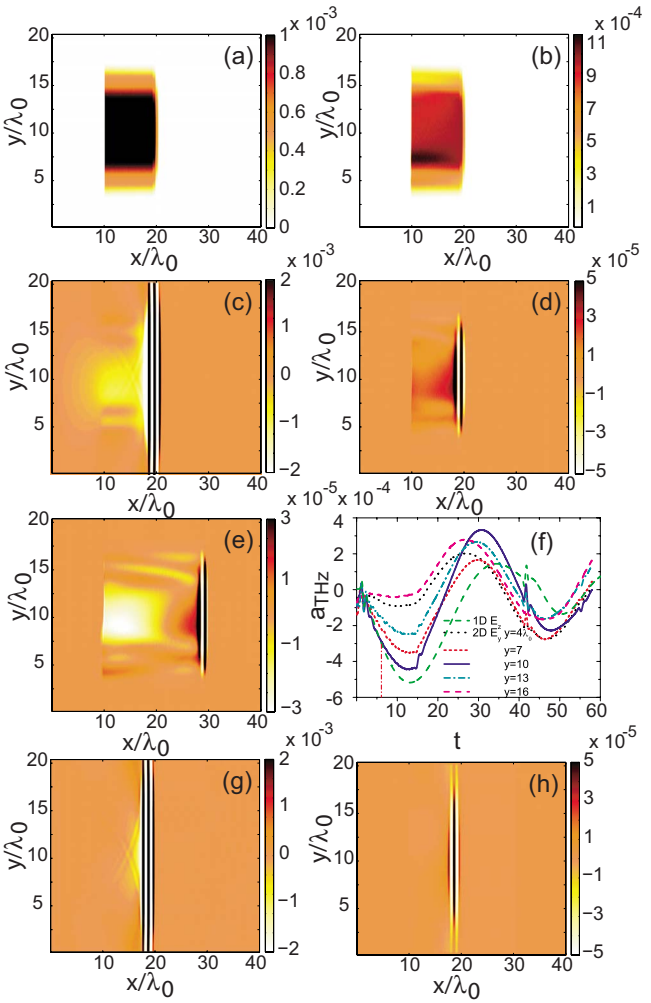

FIG. 1. (Color online) 1D and 2D PIC simulations of THz radiation. Spatial distribution of the charge density of ions $\Sigma_i q_i n_i$, q_i is the charge of the ions (a), density of electrons n_e (b), transverse electric field (c), and current (d) at $t=20T_0$ and current (e) at $t=30T_0$. The current has been normalized by $n_c ec$. (f) The temporal evolution of backward THz radiation both by 1D (green/bright-gray dashed line) and 2D simulations. The zero time has been redefined here. Spatial distribution of transverse electric field (g) and current (h) at $t=20T_0$ in the simulation without ionization.

The backward radiated THz signals both in 1D and 2D simulations are shown in Fig. 1(f). The dashed green (bright-gray) line shows the intensity of the THz electric field in the 1D simulation, and the others show the intensities at different transverse positions in the 2D simulation. The positions are labeled in the figure. As we can see from the figures, the He atoms are ionized to He^{2+} at the center of the laser beam and the average ionization degree decreases with the distance from the center. The electrons get negative velocity after the laser pulse passes, which then leads to the asymmetry in the spatial distribution of electrons as shown in Fig. 1(b) and the corresponding structure of transverse electric field and current. At $t=40T_0$ we can see the current within $10\lambda < x < 20\lambda$ has changed direction, but the current shortly after the laser pulse is still positive, which comes from the ionization. The currents in the center are uniform. However, they be-

come complicated near the edge of the laser beam, which makes the THz signal change with the transverse position. From Fig. 1(f) we can see that although the 1D result is initially coincident with the 2D simulation at the laser center, it deviates later. This means the transverse invariable character at the center of the laser beams can only be approximately kept for $5T_0$. This time is related with the laser focus size and the velocity of the electrons after the laser passed. By the way, the small peaks in Fig. 1(f) come from the reflection of the incident laser pulse at the front and rear surface of the gas boundaries. Although there is a discrepancy between the 1D and 2D simulations, generally speaking, the 1D results can still be useful to approximate the value of the THz signal. The simulation also shows, with these laser and gas parameters, the amplitude of the THz electric field can be 1.28 GV/m (normalized intensity $a_{\mathrm{THz}}=0.0004$). This is far larger than the experimental results generated by long laser pulses. Based on this, we advise one to use the ultrashort laser pulse and noble gases to be the source of THz generation.

To distinguish the contribution of the current due to ionization from the current driven by the ponderomotive force, we have made a compared simulation. In the simulation, all the parameters are the same as before except that existing plasmas with density of $0.001n_c$ has been used instead of neutral He gases. As Fig. 1(h) shows the transverse current behind the laser pulse is dramatically weakened compared with Fig. 1(d). That demonstrates the current is mainly due to initial ionization process in the laser gas interaction. Figure 1(g) shows the transverse electric field at time of $t=20T_0$, again we can see the THz field in the vacuum region is much weaker than the one in Fig. 1(c). From these, we can see THz generation by ionization current is much more important than ponderomotive force in our laser gas conditions. To get stronger THz radiation people should pay more attention to increase the ionization current.

IV. IONIZATION CURRENT AND SCALING LAWS

In this section we would like to study the dependence of the ionization current on the conditions of laser pulse and gas in detail. As we have shown above in Eq. (11), the initial ionization current itself can give us some information on the THz signal. The amplitude of the THz field is proportional to it. When we know the dependence of the ionization current on the laser and gas parameters, we can also know the dependence of THz field on them. Since the ionization and THz generation processes in the PIC code are rather complicated. To get a better insight into the process of THz generation, we developed a simplified code, in which we only calculate the ionization current by solving the ionization equation and integrating the current generated by the new born electrons.

Since the plasma density in the present case is very small, the newly released electrons are mainly dominated by the laser field. For a plane wave, the transverse momentum $\vec{p}_\perp$ of the electrons satisfies $\vec{p}_\perp - e\vec{A}_\perp/c = -e\vec{A}_\perp(t_0)/c$. Here $\vec{A}_\perp$ is the transverse vector potential of the laser pulse, t_0 is the time when the electrons released from the mother atomic or ion. After the laser pulse passed, the electrons get the velocity $\vec{v}_\perp = -e\vec{A}_\perp(t_0)/\gamma mc \equiv \vec{v}_{\perp t_0}$ with γ the relative factor. And the released electron density at that moment is $dn_e(t_0) = \Sigma_i n_i(t_0)\omega_i(t_0)dt$, where i represents the ionization order and n_i is the corresponding density of the ions. So we get the contribution of the electrons released at time of t_0 to the total ionization current $-e\vec{v}_{\perp t_0}dn_e(t_0)$. If the laser duration is significantly shorter than the plasma oscillation period which defines the evolution time of the ionization current, and the effect of the different delay time of the electrons ionized in the laser pulse is neglected, we get the total ionization current

$$\vec{J}_{\perp 0} = \frac{e^2}{mc}\sum_i \int_0^T \frac{n_i(t)\omega_i(t)\vec{A}_\perp(t)}{\gamma(t)}dt. \tag{12}$$

Here T is the duration of the incident laser pulse. So we get the initial current increasing rate $\partial J_\perp/\partial t = \vec{J}_{\perp 0}/T \approx \vec{J}_{\perp 0}\delta(t)$. The last relation comes from $\int_0^T \vec{J}_{\perp 0}/T dt = \int_0^{0+} \vec{J}_{\perp 0}\delta(t)dt$, which describes the transient ionization current.

By solving Eq. (12) and the ionization equations

$$\frac{dn_i}{n_i dt} = -\omega_i(t) \tag{13}$$

we calculate the initial ionization current with our numerical code. In our calculation, the laser pulse has a $\sin^2$ profile, the laser electric field is $a(t)=a_0 \sin^2(\pi t/T)\sin(2\pi t+\varphi_1)$, where T is the pulse duration.

We first study the case of a single long pulse. The normalized laser electric field is $a_1=0.025$ and its duration is $T=20T_0$, the laser wavelength is $\lambda=1$ μm. Figure 2(a) shows the temporal evolution of the ionization current and the electric field at a fixed point in the gas, Fig. 2(b) shows evolution of the vector potential and the ionization rate $F(\tau)=\Sigma_i n_i(\tau)\omega_i(\tau)$. As we can see, although the electrons are released two times per laser cycle at the peak point of the electric field and contribute to the ionization current, the currents have opposite directions and almost completely cancel each other after the ionization. The cancelation results from two aspects. On one hand, since the laser field is not strong enough and increases slowly with time, the ionization cannot be finished within one peak region, the ionization currents generated in the neighboring peaks negate each other. On the other hand, due to the local symmetry of the electric field at a single peak point, the ionization currents generated around the peak point also counteract each other and largely reduces the net ionization current within one ionization peak.

Considering these two aspects, different laser pulse and gas parameters can be selected to optimize the THz radiation. As Kim *et al.* have pointed out, the two-color pulse is a good selection [17]. Although the pulse is long and the ionization happens within a few cycles of the pulse front, the ionization currents do not negate each other completely, since the local symmetry of the field is broken. We show these results in Figs. 2(c) and 2(d). In this calculation the electric field satisfies $a=a_1 \sin^2(\pi t/20T_0)\sin(2\pi t+\varphi_1)+a_2 \sin^2(\pi t/20T_0)\times\sin(4\pi t+\varphi_2)$ and $\varphi_1=\varphi_2=0$, $a_1=0.017$, $a_2=0.008$. The peak value of the electric field is kept to be 0.025 as before. Actually the ionization has been finished before the laser

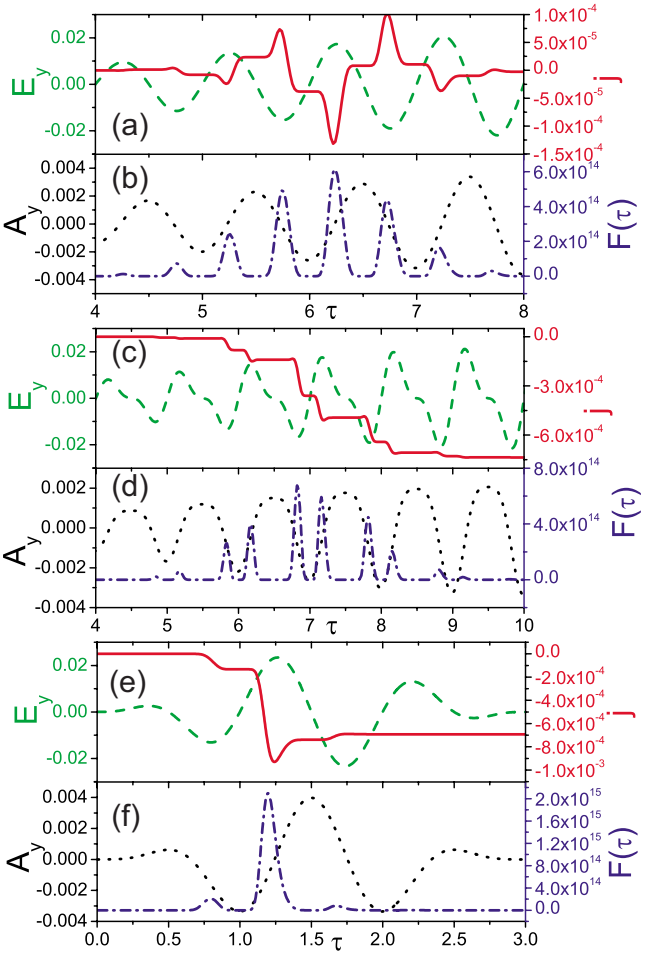

FIG. 2. (Color online) (a), (c), (e) Temporal evolution of laser electric field (dashed line) and ionization current (solid line) with different laser pulse durations and intensities. (b), (d), (f) Temporal evolution of the laser vector potential (dotted line) and the ionization rate (dash-dotted line).

peak arrived. One also sees that the net ionization current has been obviously increased when compared with the single pulse case. The reason is that the vector potential is always negative when the electrons are ionized, which makes the contributing ionization currents to have the same direction and to accumulate. This also explains the high efficiency of THz generation by use of two-color laser pulse compared with the single laser pulse as observed in the experiments by Xie *et al.* [19].

In addition to this, we can also use the ultrashort (only a few laser cycles) intense laser pulse or a pulse with a sharp increasing front which make the ionization be quickly finished within a half cycle. Then the net ionization current cannot be counteracted, and the total ionization current increases. We show the results in Figs. 2(e) and 2(f). The pulse duration is only $3T_0$, the maximum value of the laser field is the same as before. As we can see, the ionization happens immediately when the electric field is larger than the threshold value ($a_{\text{ion-th}}=0.01$) and quickly finishes before the laser peak comes. During the ionization, the vector potential is always negative. The final ionization current is almost the same as for the two-color pulse case, however, the pump

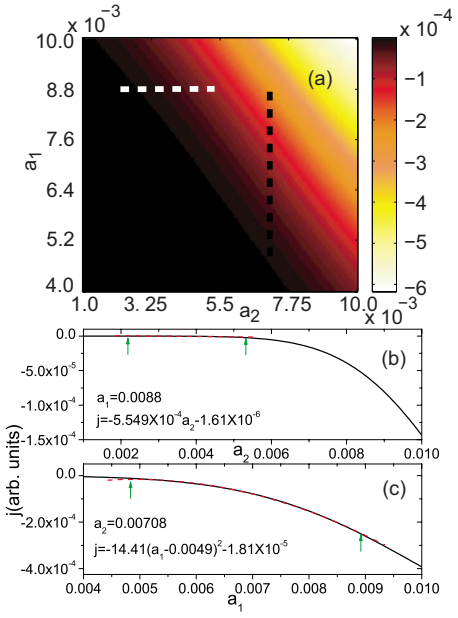

FIG. 3. (Color online) (a) Evolution of ionization current vs intensities of the two incident laser pulses. The black and white dashed lines show the parameter region of the experiments performed by Xie *et al.* [19]. (b), (c) Fit lines (red/dark-gray dashed lines) of the ionization currents. The black lines are the calculated ionization currents. The green (bright-gray) arrows mark the parameter region adopted in the experiments.

laser energy is far lower than before. As we will see later, since the ionization only happens within less than one laser cycle, the ionization current is sensitive to the carrier envelop phase (CEP), which also gives the possibility to the CEP measurement.

We have shown above that a two-color pulse can increase the ionization current, which in turn increases the THz radiation. However, the scaling laws of THz intensity on the intensity of incidence laser pulses are still unclear. In the earlier two-color pulse experiments, the mechanism has been explained by four wave mixing process, and the scaling law takes the form [19]

$$a_{\text{THz}} = \chi^{(3)} a_1^2(\omega) a_2(2\omega). \tag{14}$$

However, experimental results show that the coefficient is far larger than the third order nonlinearity originating from either/both bound electrons of ions ($\chi^{(3)}_{\text{ion}}$) or/and free electrons ($\chi^{(3)}_{\text{free electons}}$) due to ponderomotive or thermal effects [17]. Here we reconsider the experiments recently performed by Xie *et al.* using the ionization current calculations. In the simulation, we take laser and plasma parameters similar to the experiment. The laser pulse duration is $T=50T_0 \approx 133$ fs and the wavelengths are $\lambda_1=800$ nm and $\lambda_2=400$ nm. We change both the intensities of the two-color laser pulses to check the scaling. Figure 3(a) gives the dependence of the ionization current on the incident laser pulses intensity. The dashed black and white lines mark the experimental parameter range used by Xie *et al.* [19]. In Fig. 3(b), we fix the intensity of the fundamental frequency laser pulse ($a_1=0.0088$) which is close to the experiment, and vary

the intensity of the second harmonic. We revive a nearly linear fit in the parameter region covered by the experiment [between the two green (bright-gray) arrows, $0.00215 < a_2 < 0.00532$], in agreement with Eq. (14). However, when the laser intensity increases further, the scaling changes. In Fig. 3(c), we do the same calculation, but fix the intensity of the second harmonic and vary the intensity of the fundamental frequency laser pulse. Again, we can approximately get one binomial fit in the parameter region of the experiment ($a_2 = 0.00708$, $0.00468 < a_1 < 0.00893$) as Eq. (14) shows, however, the fitting line then deviates in the high intensity region.

Thus the ionization current mechanism can also well explain the experimental results and give a broader view of the dependence. From this, we can say that the nonlinear optical mechanism is not definitely the correct explanation, but maybe only by coincidence. Further experiments with higher pump energy should be carried out to check these two different mechanisms.

V. CEP MEASUREMENT BY THz GENERATION

As we pointed out before, when an ultrashort intense laser pulse interacts with gas medium, the ionization is quickly finished within less than half laser cycle and the ionization current is sensitive to the CEP. Usually the ionization only happens near the peak of the laser envelope. If we take $a_1 \sin^2(\pi t/T)\sin(2\pi t+\varphi) = a_{\text{ion-th}}$, then we get the time of ionization $t = T/2 + \delta(\varphi, T, a_{\text{ion-th}}, a_1)$, $\delta \ll T$ for $a_1 \leqslant a_{\text{ion-th}}$. The ionization current

$$
\begin{aligned}
j \propto A &= a_1 \cos(2\pi t + \varphi)[T^2 \cos(2\pi t/T)/(T^2 - 1) - 1]/4\pi \\
&\quad - a_1 T \sin(2\pi t + \varphi)\sin(2\pi t/T)/4\pi(T^2 - 1) \\
&\approx a_1 \cos[\pi T + 2\pi\delta(\varphi, T, a_{\text{ion-th}}, a_1) + \varphi]/4\pi(T^2 - 1).
\end{aligned}
$$

When T is short enough, then δ is not sensitive to φ, we can get $j \propto \cos[\pi T + \delta(T, a_{\text{ion-th}}, a_1) + \varphi]$. This means that the ionization current depends on the CEP φ as a cosine function, which makes the CEP measurement by use of THz generation possible [18].

However, since the above deduction requires the assumption: $a_1 \leqslant a_{\text{ion-th}}$, T is short enough. Otherwise $\delta = \delta(T, a_{\text{ion-th}}, a_1, \varphi)$ is the function of φ, so the relation will deviate from cosine function. Usually for a few-cycle laser pulse, T is short enough, so the amplitude of the pulse is critical for accurate CEP measurement. From $a_1 \leqslant a_{\text{ion-th}}$, we can also see that the ionization potential of the gas medium is important for the form of the relation, by selection of different gas medium (different $a_{\text{ion-th}}$) to adapt the pulse intensity (a_1) the relation can close to a cosine function.

Figure 4(a) shows evolution of the ionization current with the laser intensity and CEP. For a wide region of laser intensities ($a_1 < 0.05$), the relation curves are close to a cosine function. However, when the laser intensity increases further, this relation breaks. As shown in Fig. 4(b), there is no cosine fit for the curve of $a_1 = 0.1$, even for $a_1 = 0.05$ the discrepancy between the curve and the fit line appears. However, for He gas, the relation keeps well until $a_1 = 0.5$. We attribute this to the saturation effect of the ionization current. That means

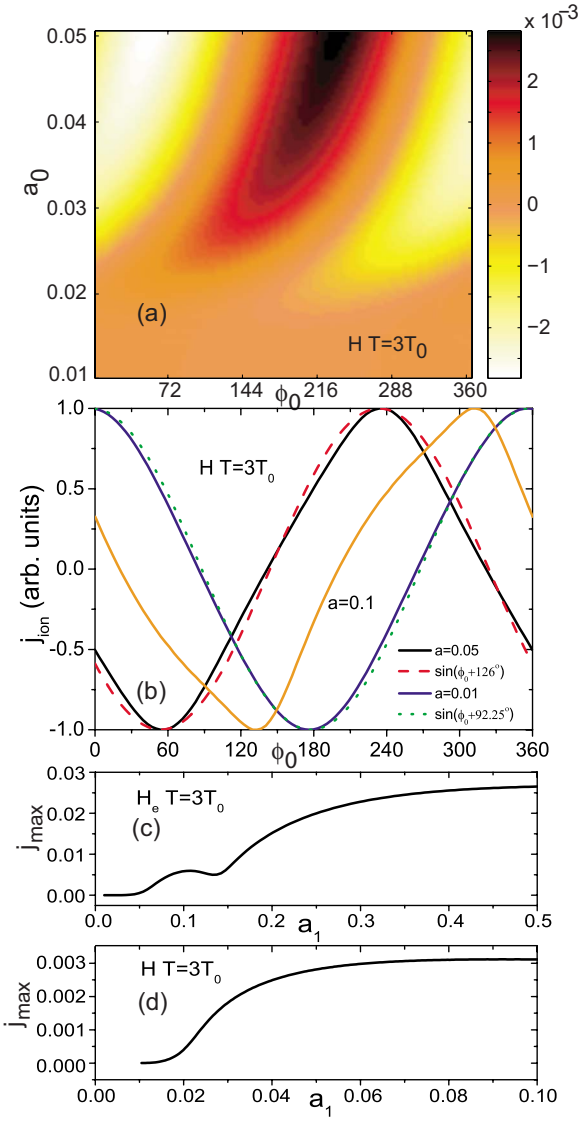

FIG. 4. (Color online) (a) Dependence of ionization current generated from H gas on the laser intensity and CEP. (b) Dependence of THz intensity on the CEP with different laser intensities. The dashed lines are the fitting lines by use of the cosine function. Dependence of maximum ionization current generated in He gas (c) and H gas (d) on the intensity of the incidence laser pulse. We can see that the saturated currents do exist.

there exists one maximum ionization current for a fixed kind of gas and pulse duration, despite the laser intensity. Figures 4(c) and 4(d) show the maximum ionization current which can be obtained from He and H gas, respectively. For every different laser intensity we change the CEP to get the maximum value of the current. It shows that the current saturates for H as $a_1 = 0.05$ and for He as $a_1 = 0.5$, respectively. They are also the maximum intensities of the laser pulses, below which the CEP can be measured by the THz signal generated by H and He gases, respectively.

VI. CONCLUSIONS

We theoretically deduce the THz radiation assuming the one dimensional geometry. Our theory explains the simula-

tion results in the one dimensional PIC simulations. Simulations also show the THz generation by ionization current mechanism is more important than the ponderomotive force mechanism in our laser gas condition. Ionization currents generated by different laser pulses and gases have been studied. We explain the high efficiency of THz radiation by use of two-color pulses and the scaling laws in the recent experiments. The proper parameter region for the CEP measurements by the use of THz generation is reconsidered and we point out the existence of the saturation of the ionization current that limits the maximum intensity of the pulse for which the CEP can be measured. By the use of a gas medium with a high ionization potential the parameter region of measurements can be broadened.

ACKNOWLEDGMENTS

M.C. acknowledges support by the Alexander von Humboldt Foundation and helpful discussions with W.M. Wang and Professor Z. M. Sheng at the Institute of Physics, China and Dr. H. C. Wu at the Max-Planck-Institut für Quantenoptik, Germany. This work is supported by the DFG programs GRK 1203 and TR18.

[1] B. Ferguson and X. C. Zhang, Nature Mater. **1**, 26 (2002).
[2] H. T. Chen, W. J. Padilla, J. M. O. Zide, A. C. Gossard, A. J. Taylor, and R. D. Averitt, Nature (London) **444**, 597 (2006).
[3] P. Sprangle, J. R. Penano, B. Hafizi, and C. A. Kapetanakos, Phys. Rev. E **69**, 066415 (2004).
[4] H. Hamster, A. Sullivan, S. Gordon, W. White, and R. W. Falcone, Phys. Rev. Lett. **71**, 2725 (1993).
[5] E. Beaurepaire, G. M. Turner, S. M. Harrel, M. C. Beard, J. Y. Bigot, and C. A. Schmuttenmaer, Appl. Phys. Lett. **84**, 3465 (2004).
[6] Z. M. Sheng, K. Mima, J. Zhang, and H. Sanuki, Phys. Rev. Lett. **94**, 095003 (2005).
[7] Z. M. Sheng, K. Mima, and J. Zhang, Phys. Plasmas **12**, 123103 (2005).
[8] H. C. Wu, Z. M. Sheng, Q. L. Dong, H. Xu, and J. Zhang, Phys. Rev. E **75**, 016407 (2007).
[9] M. H. Bae, H. J. Lee, and J. H. Choi, Phys. Rev. Lett. **98**, 027002 (2007).
[10] F. Blanchard *et al.*, Opt. Express **15**, 13212 (2007).
[11] D. J. Cook and R. M. Hochstrasser, Opt. Lett. **25**, 1210 (2000).
[12] S. Tzortzakis *et al.*, Opt. Lett. **27**, 1944 (2002).
[13] Y. Liu, A. Houard, B. Prade, S. Akturk, A. Mysyrowicz, and V. T. Tikhonchuk, Phys. Rev. Lett. **99**, 135002 (2007).
[14] C. D'Amico, A. Houard, M. Franco, B. Prade, A. Mysyrowicz, A. Couairon, and V. T. Tikhonchuk, Phys. Rev. Lett. **98**, 235002 (2007).
[15] C. D. Amico, A. Houard, S. Akturk, Y. Liu, J. Le Bloas, M. Franco, B. Prade, A. Couairon, V. T. Tikhonchuk, and A. Mysyrowicz, New J. Phys. **10**, 013015 (2008).
[16] V. B. Gildenburg and N. V. Vvedenskii, Phys. Rev. Lett. **98**, 245002 (2007).
[17] K. Y. Kim, J. H. Glownia, A. J. Taylor, and G. Rodriguez, Opt. Express **15**, 4577 (2007).
[18] M. Kress *et al.*, Nat. Phys. **2**, 327 (2006).
[19] X. Xie, J. M. Dai, and X. C. Zhang, Phys. Rev. Lett. **96**, 075005 (2006).
[20] M. Chen, Z. M. Sheng, J. Zheng, Y. Y. Ma, and J. Zhang, Chin. J. Comput. Phys. **25**, 43 (2008).
[21] M. Chen, Z. M. Sheng, Y. Y. Ma, and J. Zhang, J. Appl. Phys. **99**, 056109 (2006).
[22] H. C. Wu, J. Meyer-ter Vehn, and Z. M. Sheng, New J. Phys. **10**, 043001 (2008).
[23] B. M. Penetrante and J. N. Bardsley, Phys. Rev. A **43**, 3100 (1991).
[24] A. J. Kemp, R. E. W. Pfund, and M. ter Vehn J., Phys. Plasmas **11**, 5648 (2004).